

Photonic Amplification by a Singlet-State Quantum Chain Reaction in the Photodecarbonylation of Crystalline Diarylcyclopropenones

Gregory Kuzmanich, Matthew N. Gard, and Miguel A. Garcia-Garibay*

Department of Chemistry and Biochemistry, University of California,
Los Angeles, California 90024-1569

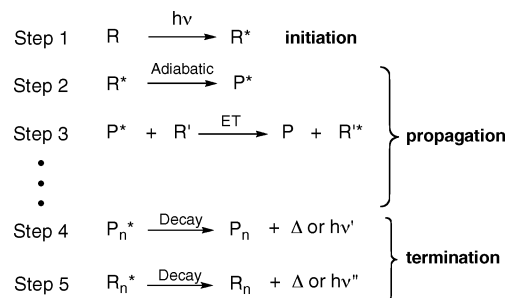
Received May 28, 2009; E-mail: mgg@chem.ucla.edu

Abstract: The photochemical decarbonylation of diphenylcyclopropenone (DPCP) to diphenylacetylene (DPA) proceeds with remarkable efficiency both in solution and in the crystalline solid state. It had been previously shown that excitation to the second electronic excited state (S_2) of DPCP in solution proceeds within ca. 200 fs by an adiabatic ring-opening pathway to yield the S_2 state of DPA, which has a lifetime of ca. 8 ps before undergoing internal conversion to S_1 (Takeuchi, S.; Tahara, T. *J. Chem. Phys.* **2004**, *120*, 4768). More recently, we showed that reactions by excitation to S_2 in crystalline solids proceed by a quantum chain process where the excited photoproducts transfer energy to neighboring molecules of unreacted starting material, which are able to propagate the chain. Quantum yields in crystalline suspensions revealed values of $\Phi_{\text{DPCP}} = 3.3 \pm 0.3$. To explore the generality of this reaction, and recognizing its potential as a photonic amplification system, we have synthesized nine crystalline diarylcyclopropenone derivatives with phenyl, biphenyl, naphthyl, and anthryl substituents. To quantify the efficiency of the quantum chain in the crystalline state, we determined the quantum yields of reaction for all of these compounds both in solution and in nanocrystalline suspensions. While the quantum yields of decarbonylation in solution vary from $\Phi = 0.0$ to 1.0, seven of the nine new structures display quantum yields of reaction in the solid that are above 1. The chemical amplification that results from efficient energy transfer in the solid state, analyzed in terms of the quantum yields determined in the solid state and in solution ($\Phi_{\text{cryst}}/\Phi_{\text{soln}}$), reveals quantum chain amplification factors that range from 3.2 to 11.0. The remarkable mechanical response of the solid-to-solid reaction previously documented with macroscopic crystals, where large single-crystalline specimens turn into fine powders, was investigated at the nanometer scale. Experiments with dry crystals of DPCP analyzed by atomic force microscopy showed the formation of DPA in the form of isolated crystalline specimens ca. 35 nm in size.

Introduction

Quantum chain reactions are characterized by the formation of more than one product molecule per photon of light absorbed (Scheme 1). Unlike normal chain reactions involving radicals¹ and other ground-state reactive intermediates,² quantum chain reactions involve chain carriers in the excited state.^{3,4} The conditions required for a quantum chain reaction were first

Scheme 1



documented by Hammond.⁴ Quantum chain reactions start by formation of an excited state (Step 1, Scheme 1) and are followed by a relatively uncommon propagation step (Step 2) involving an adiabatic photochemical reaction that gives rise to the photoproduct in the excited state.⁵ This is followed by energy transfer to a new ground-state reactant that propagates the chain (Step 3). Termination occurs when either the excited-

- (1) (a) Moad, G.; Solomon, D. H. *The Chemistry of Radical Polymerization*, 2nd ed.; Elsevier: Oxford, UK, 2006. (b) Griesbeck, A. G.; Hoffmann, N.; Warzecha, K.-D. *Acc. Chem. Res.* **2007**, *40*, 128.
- (2) (a) Marquez, C. A.; Wang, H.; Fabbretti, F.; Metzger, J. O. *J. Am. Chem. Soc.* **2008**, *130*, 17208. (b) Maruyama, T.; Mizuno, Y.; Shimizu, I.; Suga, S.; Yoshida, J.-I. *J. Am. Chem. Soc.* **2007**, *129*, 1902. (c) Norton, J. E.; Olson, L. P.; Houk, K. N. *J. Am. Chem. Soc.* **2006**, *128*, 7835. (d) Baciocchi, E.; Bietti, M.; Putignani, P.; Steenken, S. *J. Am. Chem. Soc.* **1996**, *118*, 5952. (e) Matmour, R.; More, A. S.; Wadgaonkar, P. P.; Gnanou, Y. *J. Am. Chem. Soc.* **2006**, *128*, 8158. (f) Waddell, W. H.; Lee, C. H. *J. Am. Chem. Soc.* **1982**, *104*, 5804.
- (3) A quantum chain reaction was first suggested in the isomerization of 1,5,9-cyclododecatriene, but it was discarded on the basis of energetic arguments. Crandall, J. K.; Mayer, C. F. *J. Am. Chem. Soc.* **1967**, *89*, 4374.
- (4) The first documented quantum chain reaction involves the triplet sensitized photoisomerization of 2,4-hexadiene. Hyndman, H. L.; Monroe, B. M.; Hammond, G. S. *J. Am. Chem. Soc.* **1969**, *91*, 2852.

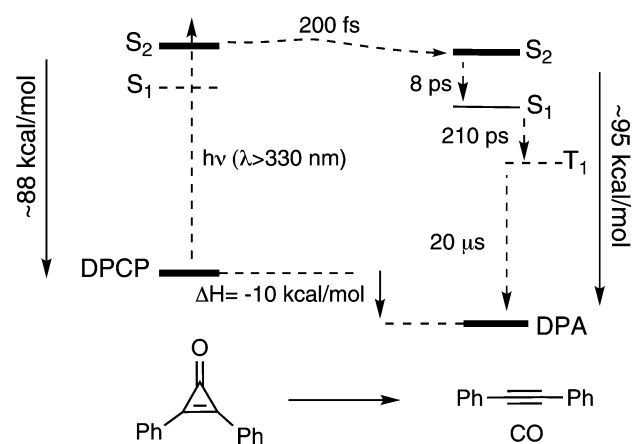
- (5) Turro, N. J.; McVey, J.; Ramamurthy, V.; Lechtken, P. *Angew. Chem., Int. Ed. Engl.* **1979**, *18*, 572–586.

state reactant or product undergoes thermal or radiative decay (Step 4 and/or Step 5).

As recently suggested by Gillmore et al., quantum amplified reactions with long propagation lengths would be ideal for the amplification of photonic signals, with potential in lithographic and sensing applications.⁶ Most signal amplification strategies developed to date deal with the optimal capture and use of every photon absorbed, as exemplified by Swager's molecular wire approach⁷ and several related strategies.⁸ In contrast, quantum chain reactions generate more than one chemical event per photon, and harnessing their potential would be highly desirable. Recent examples of quantum chain processes in materials science include the use of polymeric materials undergoing changes in refractive index as a result of radical ion chains,⁶ super-high-spin magnetic polycarbenes,^{8h} or triplet quantum chain⁹ reactions of Dewar benzene to Hückel benzene.

Despite their promising nature, the control of quantum chain reactions represents a significant challenge, especially as it pertains to the propagation events in Scheme 1. Limitations arise from the relatively small number of adiabatic reactions developed at this time (Step 2) and from the challenges involved in designing an efficient energy-transfer process (Step 3). If one considers reactions that occur in solution, long chain reactions will require excited states with long lifetimes and high reactant concentrations. It is therefore not surprising that almost all known quantum chain reactions occur in triplet states. Examples include cis–trans isomerization of alkenes and polyenes,^{4,10,11} decomposition of dioxetanes to ground- and excited-state ketones,^{12,13} and several bond-valence isomerizations.^{5,9,14} In fact, singlet-state quantum chains are severely limited by the short excited-state lifetimes, which make energy transfer by diffusion mechanisms very unlikely. Adiabatic reactions that take place in the singlet state have been established by detecting

Scheme 2



the fluorescence¹⁵ or transient absorption of the excited photoproduct rather than by observation of a quantum chain with quantum yields of product formation that are greater than 1. It should be noted that some adiabatic reactions, such as the fragmentation of dioxetanes and the bond-valence isomerization of Dewar naphthalene, may take place along both the singlet and triple manifolds. Other reactions have been reported to occur specifically along the singlet or triplet state.⁵

Recognizing that energy transfer in crystalline solids may take place on a sub-picosecond time scale,¹⁶ we recently proposed that crystalline solids should be ideal candidates for quantum chain processes, increasing the efficiency of Step 3 in Scheme 1. It seems reasonable that ultrafast energy transfer will make quantum chains possible even for the shortest-lived singlet states. On the basis of our recent experience with the photodecarbonylation of crystalline ketones¹⁷ and reports of an adiabatic photodecarbonylation of diphenylcyclopropenone (DPCP) to diphenylacetylene (DPA),¹⁸ we decided to investigate this reaction as a possible test system.¹⁹ As discussed below, an adiabatic reaction along an upper excited singlet state represents one of the most challenging systems for quantum chains, which can set the stage for rapid future progress.

Transient absorption studies in solution, starting in the early 1990s by Hirata et al.,^{18c} suggested an adiabatic reaction from the second excited state, S₂-DPCP, which has been recently estimated to occur with a time constant of ca. 200 fs, as illustrated in Scheme 2.^{18a} While there has been some debate

- (6) Gillmore, J. G.; Neiser, J. D.; McManus, K. A.; Roh, Y.; Dombrowski, G. W.; Brown, T. G.; Dinnocenzo, J. P.; Farid, S.; Robello, D. R. *Macromolecules* **2005**, *38*, 7684–7694.
- (7) Swager, T. M. *Acc. Chem. Res.* **1998**, *31*, 201.
- (8) Photon capture and transport by conjugated polymers has been applied in many different contexts. (a) Swager, T. M. *Acc. Chem. Res.* **2008**, *41*, 1181. (b) Mitrovics, J.; Ulmer, H.; Weimar, U.; Göpel, W. *Acc. Chem. Res.* **1998**, *31*, 307. (c) Albert, K. J.; Lewis, N. S.; Schauer, C. L.; Sotzing, G. A.; Stitzel, S. E.; Vaid, T. P.; Walt, D. R. *Chem. Rev.* **2000**, *100*, 2595. (d) Vetrichelvan, M.; Nagarajan, R.; Valiyaveetil, S. *Macromolecules* **2006**, *39*, 8303. (e) Liu, Y.; Mills, R. C.; Boncella, J. M.; Schanze, K. S. *Langmuir* **2001**, *17*, 7452. (f) Hong, J. W.; Gaylord, B. S.; Bazan, G. C. *J. Am. Chem. Soc.* **2002**, *124*, 11868. (g) Jones, R. M.; Bergstedt, T. S.; McBranch, D. W.; Whitten, D. G. *J. Am. Chem. Soc.* **2001**, *123*, 6726. (h) Matsuda, K.; Nakamura, N.; Takahashi, K.; Inoue, K.; Koga, N.; Iwamura, H. *J. Am. Chem. Soc.* **1995**, *117*, 5550.
- (9) (a) Merkel, P. B.; Roh, Y.; Dinnocenzo, J. P.; Robellow, D. R.; Farid, S. *J. Phys. Chem. A* **2007**, *111*, 1188. (b) Ferrar, L.; Mis, M.; Dinnocenzo, J. P.; Fardid, S.; Merkel, P. B.; Robello, D. R. *J. Org. Chem.* **2008**, *73*, 5683.
- (10) (a) Saltiel, J.; Dmitrenko, O.; Pillai, Z. S.; Klima, R.; Wang, S.; Wharton, T.; Huang, Z.-N.; van de Burgt, L. J.; Arranz, J. *Photochem. Photobiol. Sci.* **2008**, *7*, 566. (b) Saltiel, J.; Dmitrenko, O.; Reischl, W.; Bach, R. D. *J. Phys. Chem. A* **2001**, *105*, 3934. (c) Saltiel, J.; Wang, S.; Ko, D.-H.; Groming, D. A. *J. Phys. Chem. A* **1998**, *102*, 5383. (d) Saltiel, J.; Townsend, D. E.; Skyes, A. *J. Am. Chem. Soc.* **1973**, *95*, 5968.
- (11) (a) Karatus, T.; Tsuchiya, M.; Arai, T.; Sakuragi, H.; S.; Tokumaru, K. *Bull. Chem. Soc. Jpn.* **1994**, *67*, 3030. (b) Möllerstedt, H.; Wennerström, O. *J. Photochem. Photobiol. A* **2001**, *139*, 37.
- (12) Turro, N. J.; Waddell, W. H. *Tetrahedron Lett.* **1975**, *25*, 2069.
- (13) (a) Zharinova, E. V.; Voloshin, A. I.; Kazakov, V. P. *J. Mol. Liq.* **2001**, *91*, 237–243. (b) Kazakov, V. P.; Voloshin, A. I.; Shavaleev, N. M. *J. Photochem. Photobiol. A* **1998**, *119*, 177.
- (14) (a) Turro, N. J.; Ramamurthy, V.; Katz, T. J. *Nouv. J. Chim.* **1977**, *1*, 363. (b) Lechtken, P.; Yekta, A.; Shore, N. E.; Steinmetzer, H. C.; Waddell, W. H.; Turro, N. J. *Z. Phys. Chem.* **1976**, *101*, 79.

- (15) (a) Carr, R. V.; Kim, B.; McVey, J. K.; Yang, N. C.; Gerhartz, W.; Michl, J. *Chem. Phys. Lett.* **1976**, *39*, 57. (b) Yang, N. C.; Carr, R. V.; Li, E.; McVey Rice, J. *Chem. Phys. Lett.* **1976**, *39*, 57.
- (16) (a) Powel, R. C.; Soos, A. G. *J. Lumin.* **1975**, *11*, 1. (b) Swenberg, C. E.; Gaecintov, N. E. In *Organic Molecular Photophysics*; Birks, J. B. Ed.; John Wiley and Sons: London, 1973. (c) Yoon, Z. S.; Yoon, M.-C.; Kim, D. *J. Photochem. Photobiol. C* **2005**, *6*, 249. (d) Ahrens, M. J.; Sinks, L. E.; Rytchinski, B.; Liu, W.; Jones, B. A.; Giaimo, J. M.; Gusev, A. V.; Goshe, A. J.; Tiede, D. M.; Wasielewski, M. R. *J. Am. Chem. Soc.* **2004**, *126*, 8284.
- (17) (a) Campos, L. M.; Garcia-Garibay, M. A. In *Reviews of Reactive Intermediate Chemistry*; Platz, M. S.; Jones, M., Moss, R., Eds.; Wiley-Interscience: Hoboken, NJ, 2007. (b) Mortko, C. J.; Garcia-Garibay, M. A. *Top. Stereochem.* **2006**, *25*, 205–253. (c) Garcia-Garibay, M. A. In *The Handbook for Organic Photochemistry and Photobiology*; Horspool, W., Ed.; CRC Press: Boca Raton, FL, 2003.
- (18) (a) Takeuchi, S.; Tahara, T. *J. Chem. Phys.* **2004**, *120*, 4768. (b) Terazima, M.; Hara, T.; Hirota, N. *Chem. Phys. Lett.* **1995**, *246*, 577. (c) Hirata, Y.; Okada, T.; Mataga, N.; Nomoto, T. *J. Phys. Chem.* **1992**, *193*, 287.
- (19) Kuzmanich, G.; Natarajan, A.; Chin, K.; Veerman, M.; Mortko, C.; Garcia-Garibay, M. A. *J. Am. Chem. Soc.* **2008**, *130*, 1140.

over the detailed spectral assignments,²⁰ the time constant for internal conversion from S₂-DPA to S₁-DPA was estimated to be 8 ps. This is followed by intersystem crossing to T₁-DPA in ca. 210 ps and by decay to the ground-state product in ca. 20 μs. The same studies concluded that excitation to S₁-DPCP proceeds by a conventional non-adiabatic reaction to the ground state of DPA.¹⁸ In addition to forming an excited-state photo-product, the feasibility of a quantum chain process depends on the energetics of energy transfer. In the cases of DPCP and DPA, one can estimate from the spectrum that the second excited-state energies (S₂-DPCP and S₂-DPA) are 88 and 95 kcal/mol, respectively, which makes energy transfer from the excited-state product to the ground-state reactant exothermic, and therefore viable. Notably, the greater S₂-S₀ energy gap for DPA is determined by the lower energy content of its ground state, which is ca. 10 kcal/mol more stable than that of the strained ketone (Scheme 2). It is interesting to note that these values make the adiabatic reaction exothermic by ca. 3.0 kcal/mol. Evaluation of the factors required for a quantum chain in the case of DPCP shows that the main limitation should come from the short lifetime of S₂-DPA, which gives only ca. 8 ps to transfer its excitation energy to a nearby reactant molecule. If reacted as a molecular solid, where singlet excitons have hopping times of ca. 1–2 ps, one may expect that every photon initiating the ring-opening reaction of a DPCP molecule should be able to “tag” as many as 4–8 reactant molecules before one of them undergoes internal conversion to the first excited state (S₁), which no longer satisfies the energetic requirements for energy transfer. Alternatively, the mechanism could involve an excited state delocalized throughout the crystal, which could cause several molecules to react.^{8b} To demonstrate this, one must measure the quantum yield of the solid-state reaction and unequivocally show that is greater than one ($\Phi_{\text{rxn}} > 1.0$). In agreement with these expectations, we recently showed that macroscopic specimens of DPCP undergo a remarkably efficient reaction that transforms single crystals into fine powders of DPA within minutes.¹⁹ More importantly, quantum yield determinations with nanocrystalline suspensions using dicumyl ketone (DCK, $\Phi_{\text{rxn}} = 0.2$) as an internal actinometer revealed an average quantum yield of $\Phi_{\text{rxn}} = 3.3$ when DPCP is excited to S₂ in the crystalline state.¹⁹

Recognizing the potential of a photoinduced amplification system that unveils highly emissive and charge-transporting diarylacetylenes,²¹ we decided to explore the scope of the quantum chain reaction. In this paper, we describe the synthesis, nanocrystal formation, nanocrystal photochemistry, and solution and solid-state quantum yield determinations of nine symmetric diarylcyclopropenones, **1b–1j**. The formation and characterization of nanocrystals for all DPCP derivatives was deemed essential to determine reliable solid-state quantum yields. Included in Table 1 are structures with aryl substituents that include *para*-substituted benzenes (**1b**, **1h–1j**), bibenzyl (**1e**), biphenyl (**1f**), two naphthalenes (**1c** and **1d**), and a 9-anthracene derivative (**1g**). While efficient quenching mechanisms were

deduced from the observed photostability of the 9-anthryl (**1g**) and *p*-iodophenyl (**1h**) derivatives, significant quantum chain processes were determined for all the other structures.

Results and Discussion

Synthesis of Diarylcyclopropenone Derivatives. Derivatives **1b–1h** were prepared by Friedel–Crafts alkylation of the corresponding aromatic moiety with tetrachlorocyclopropenone in DCM at –78 °C.²² The resulting products were purified by column chromatography (silica gel, 4:1 hexane:acetone) followed by one or more recrystallizations in hexane with ca. 5% acetone or dichloromethane. As indicated in Table 1, isolated yields of the pure product varied from 40% to 65%. Samples of the bisphenol **1i** were prepared from the *p*-methoxy analogue **1b**, as shown in Scheme 3, and were purified in a similar manner. The crystalline salt **1j** was obtained by dissolving **1i** in triethylamine, consistent with a remarkably high acidity for the latter, which was later confirmed by spectrophotometric methods and by titration of **1i**. All cyclopropenone derivatives were characterized by having the ¹H NMR signal of the hydrogens meta to the electron-withdrawing cyclopropenone at $\delta > 8$ ppm and the ¹³C NMR signal of the carbonyl carbon distinct at ca. 165 ppm. While these compounds were all characterized by conventional spectroscopic methods that agree with literature reports,²³ we reassigned the structure of **1f** as illustrated in Table 1. A lower symmetry structure with an *o*-methoxy linkage, rather than the suggested 4-(*p*-anisyl)phenyl derivative, is determined by the ¹H and ¹³C NMR spectra, which include the presence of an isolated ¹H resonance at 8.21 ppm that integrates for only one hydrogen, and by the 15 rather than 10 signals in the ¹³C NMR (Supporting Information). All of the cyclopropenone derivatives are crystalline powders with high melting points, which help ensure that the solid-state reaction does not take place in the melt. The parent DPCP has the lowest melting point, 87 °C. All known derivatives had melting points identical to those reported in the literature, typically between 130 and 160 °C, as shown in Table 1. The 9-dianthryl derivative **1e** and the crystalline salt **1j** decomposed before melting at T ≥ 350 °C.

While derivatives **1a**, **1b**, **1h**, and **1j** form white microcrystalline powders, those of the more conjugated **1c**, **1d**, and **1f** are pale yellow, and those of **1g** are vibrant red. All crystalline powders, except for **1g**, were soluble in methanol, chloroform, and acetone. The dianthryl compound **1g** was highly insoluble in all solvents tested, and we decided to acquire its ¹³C NMR spectra by solid-state CPMAS NMR to make sure that it conforms to the other structures (Supporting Information). The CPMAS clearly shows the presence of the distinct carbonyl carbon at 159 ppm along with the other cyclopropene carbons at ca. 146 ppm. Additionally, the only other carbon signals in the spectrum are in the aromatic region, 116–127 ppm, similar to those of the other compounds in solution. Judging by its UV–vis and ¹H NMR spectra, solutions of bisphenol **1i** in methanol, water, or acetone exist in equilibrium between the neutral and the mono-dissociated forms. The addition of triethylamine results in formation of a quaternary ammonium salt, characterized by a downfield shift of 0.13 and an upfield shift of 0.11 ppm in the ¹H NMR for the aromatic signals at

(20) Poloukhine, A.; Popik, V. V. *J. Phys. Chem. A* **2006**, *110*, 1749.

(21) (a) Bunz, W. H. F. *Chem. Rev.* **2000**, *100*, 1605. (b) Nesterov, E. E.; Zhu, Z.; Swager, T. M. *J. Am. Chem. Soc.* **2005**, *127*, 10083. (c) Meier, H. *Angew. Chem., Int. Ed.* **2005**, *44*, 2482. (d) Levitus, M.; Schmieder, K.; Ricks, H.; Shimizu, K. D.; Bunz, W. H. F.; Garcia-Garibay, M. A. *J. Am. Chem. Soc.* **2001**, *123*, 4259. (e) Stapleton, J. J.; Harder, P.; Daniel, T. A.; Reinard, M. D.; Yao, Y.; Price, D. W.; Tour, J. M.; Allara, D. L. *Langmuir* **2003**, *19*, 8245. (f) Samori, S.; Tojo, S.; Fujitsuka, M.; Spitler, E. L.; Haley, M. M.; Majima, T. *J. Org. Chem.* **2007**, *72*, 2785.

(22) West, R.; Zecher, D. C.; Goyert, W. *J. Am. Chem. Soc.* **1970**, *92*, 149.

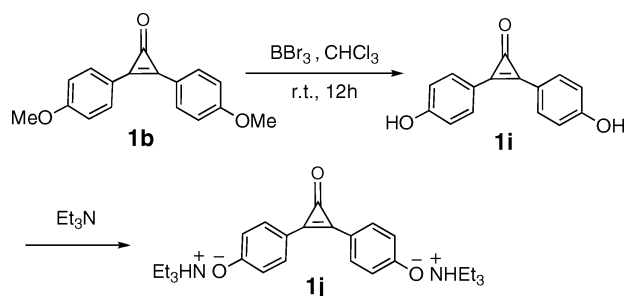
(23) (a) Urdabayev, N. K.; Poloukhine, A.; Popik, V. V. *Chem. Commun.* **2006**, *4*, 454. (b) Poloukhine, A.; Popik, V. V. *J. Org. Chem.* **2003**, *68*, 7833.

Table 1. Synthetic Isolated Yields, Melting Points, UV–Vis Data, Photochemical Quantum Yields in Solution and in Crystalline Suspension, and Quantum Yield Amplification Values for Several DPCP Derivatives

Ar + 2 eq $\xrightarrow[\text{H}_2\text{O}]{\text{AlCl}_3, \text{DCM}, -78^\circ\text{C} - \text{rt}}$ 1 eq **1a-j** $\xrightarrow[\text{Suspension or solution}]{h\nu}$ **2a-j**

Entry	Substrate (Ar)	Yield (%)	Melting Point (°C)	λ_{max} (nm)	Quantum Yield Susp	Quantum Yield Soln	Quantum Yield Amplification
1a		- ^a	87	345, 325	3.3±0.3 ^b	1.00 ^c	3.3
1b		65	121	340, 364, 347	2.74±0.28	0.24 ^d	11.4
1c		41	172	383, 364, 347	2.23±0.47	0.7 ^d	3.2
1d		46	162	360, 347	1.52±0.16	0.46 ^e	3.3
1e		60	216	339, 318, 305	1.22±0.04	0.22	5.6
1f		56	220	350, 306	2.74±0.05	0.5 ^e	5.5
1g		51	>350	490, 372	0	0.01-0.02 ^{ef}	n.a.
1h		58	189	334	0	0	n.a.
1i		- ^g	163	360, 292	1.62±0.16	0.27	6
1j		- ^g	>350	381, 365	0.87±0.09	0.22	4

^a Commercially available. ^b Reference 18. ^c Reference 11. ^d Reference 23b. ^e Reference 23a. ^f Reference 12. ^g See Scheme 3 for synthesis and yields.

Scheme 3

6.91 and 7.80 ppm, respectively. The dianionic nature of **1j** was also confirmed by showing that it has a UV–vis spectrum that is identical to that of a sample prepared by deprotonation with 2 equiv of LHMDS. The UV–vis spectrum of the dianion is significantly red-shifted relative to that of **1i**. The onset of absorption is at 410 nm for **1j** and 360 nm for **1i** (Supporting Information). Determinations of the $\text{p}K_{\text{a}}$ of **1i** by methanolic titrations with 0.1 M KOH revealed a single value of $\text{p}K_{\text{a}} = 5.48$ for the apparent double deprotonation (see Supporting Information for details). With this value, the acidity of **1i**

compares favorably with that of 2,4-dinitrophenol, which has $\text{p}K_{\text{a}} = 4.09$,²⁴ but is not as acidic as picric acid (2,4,6-trinitrophenol), with $\text{p}K_{\text{a}} = 0.3$.²⁵ A ca. 30 nm red-shift was observed on going from the spectrum of the phenol to that of the double salt both in solution and in the crystalline salt.

Preparation and Characterization of Nanocrystalline Suspensions. We have shown that suspensions of nanocrystalline solids offer significant advantages over large single crystals and dry powders for photochemical studies.²⁶ As particle sizes approach the wavelength of individual photons, samples can be excited in a nearly homogeneous manner, avoiding problems of penetration depth and possible filtering effects by strongly absorbing photoproducts.²⁷ Nanocrystalline suspensions are also ideal for large-scale solid-state photochemical reactions using

(24) Barcza, L.; Buvári-Barcza *J. Chem. Educ.* **2003**, *80*, 822.

(25) Jin, C.-M.; Ye, C.; Piekarski, C. *Eur J. Inorg. Chem.* **2005**, *18*, 3760.

(26) Veerman, M.; Resendiz, M. J. E.; Garcia-Garibay, M. A. *Org. Lett.* **2006**, *8*, 2615–2617.

(27) Resendiz, M. J. E.; Taing, J.; Garcia-Garibay, M. A. *Org. Lett.* **2007**, *9*, 4351–4354.

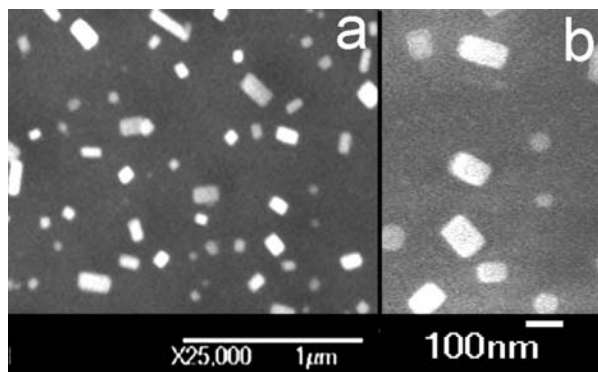


Figure 1. (a) SEM image of DPCP isolated nanocrystals showing crystals of ca. 50–200 nm on an alkane monolayer on a Si surface. (b) 4.6× magnification of the right portion of panel a.

flow reactors and for spectrophotometric analysis by transmission methods.²⁸

The simplest and most efficient method for the preparation of nanocrystalline suspensions is the reprecipitation method initially pioneered by Kasai et al.,²⁹ which produces nanocrystals between ca. 50 and 600 nm in size for a variety of substrates. In order to determine the solid-state reactivity and quantum yields of reaction for the DPCP derivatives in Table 1, we typically used 1.6–2.6 mg (0.064 mmol) of each compound dissolved in a minimal amount of acetone or methanol. These solutions were added rapidly via a micropipet into a test tube containing 9 mL of vortexing H₂O with 1/20th of the critical micelle concentration (cmc) of either cetyltrimethylammonium bromide (CTAB) or sodium dodecyl sulfate (SDS).³⁰ The resulting milky suspensions were sonicated for 40 min at 60 °C to ensure that no acetone remained in the sample. Given that analogous suspensions were obtained from all diarylcyclopropanone derivatives, we decided to carry out a thorough characterization with the parent compound, assuming that it would be a reasonable model for the others in the set. Using X-ray powder diffraction of centrifuged nanoparticles, we confirmed that the nanocrystalline suspensions adopt one of the polymorphs observed with bulk DPCP (see Supporting Information). Notably, while it is well known that DPCP forms hydrated³¹ and anhydrous³² forms by slow evaporation from water-saturated and dry benzene, respectively, it seemed surprising that the anhydrous form would be obtained upon precipitation in water. As in other cases reported in the literature, we hypothesize that this apparent anomaly simply indicates both that nucleation and growth under these conditions are kinetically controlled and that the incorporation of water requires thermodynamic equilibrium.³³

Dynamic light scattering (DLS) studies performed on a DPCP suspension with a 4×10^{-5} M loading revealed average particle sizes between 100 and 250 nm. As illustrated in Figure 1, DPCP

nanocrystals obtained by the reprecipitation protocol were analyzed by atomic force microscopy (AFM) and scanning electron microscopy (SEM) to verify the particle size and the crystallinity of the nanospecimens. Both isolated crystals and aggregates were observed from suspensions deposited on an alkane-terminated monolayer on a silicon wafer.³⁴ Figure 1a shows isolated DPCP nanocrystals with sizes ranging between ca. 100 and 200 nm, in general agreement with the DLS results from the fluid suspension. The SEM image also shows that the particles are clearly faceted and crystalline.

Photochemical Reactivity in Polycrystalline Powders. We have suggested that dissociative photochemical reactions in crystalline solids can be engineered in a reliable manner by selecting high-melting substrates with exothermic bond-cleavage reactions^{17,35} that have no easy radical recombination and no quenching processes. It seemed reasonable to us that the photodecarbonylation of simple DPCP derivatives should be quite general. Photochemical experiments with cyclopropanones **1a–1j** were carried out at 298 K with a mercury arc Hanovia lamp using a $\lambda > 290$ nm (Pyrex) filter or with the 312 nm bulbs of a Rayonet reactor. Samples irradiated in solution by ¹H NMR and in bulk polycrystalline powders revealed that most compounds reacted to completion to give the corresponding diaryl acetylene powders within 60 min. The only exceptions were compounds **1g** and **1h**. Samples of bis(*p*-iodophenyl)cyclopropanone **1h** were photochemically stable in methanol, chloroform, nanocrystalline suspension, and dry powders. We interpret this result as indicative of a very efficient singlet-state deactivation by the iodine heavy-atom effect.³⁶ Similarly, samples of bis(9-anthryl)cyclopropanone **1g** irradiated with $\lambda \geq 290$ nm were stable in suspensions and in dry solids, but they are modestly reactive in solution. Reaction quantum yields of 0.02 and 0.01 have been previously reported in dilute toluene and methylene chloride, respectively.^{37,38}

Fluorescence measurements with **1g** in CH₂Cl₂ solutions and nanocrystalline suspensions yielded similar spectra. Identical absorption (Supporting Information) and fluorescence excitation (Figure 2) spectra are indicative of a sample with no other fluorescent impurities. The two spectra are characterized by a structureless low-energy transition with $\lambda_{\text{max}} = 465$ nm, having two shoulders at lower (445 nm) and higher (515) wavelengths in the case of the solid suspension. As expected, photochemical excitation in this band results in no decarbonylation reaction in solution. Previous studies with several dianthryl ethenes by Becker et al., including **1g**, suggested that the lowest-energy transition in these chromophores is due to an intramolecular excimer, which is dominant in solution and in the solid state.^{37,38} Thus, it is likely that the solution reactivity observed upon excitation of **1g** with short wavelengths is due to a very fast adiabatic reaction from an upper excited state largely localized in the DPCP chromophore. The lack of reactivity in the solid state under similar conditions suggests a very fast internal conversion within the bis(anthracene)-centered lowest excited state. We considered that the lack of reactivity in crystals of **1g**

(28) Chin, K. K.; Natarajan, A.; Gard, M.; Campos, L. M.; Johansen, E.; Shepherd, H.; Garcia-Garibay, M. A. *Chem. Commun.* **2007**, 4266–4268.

(29) Kasai, H.; Nalwa, H. S.; Oikawa, H.; Okada, S.; Matsuda, H.; Minami, N.; Kakuta, A.; Ono, K.; Mukoh, A.; Nakanishi, H. *Jpn. J. Appl. Phys.* **1992**, *31*, 1132.

(30) Medium-sensitive spectral measurements can be used to distinguish between solid suspension and micelles before irradiation.¹⁹

(31) Tsukada, H.; Shimanouchi, H.; Sasada, Y. *Tetrahedron Lett.* **1973**, *14*, 2455.

(32) Tsukada, H.; Shimanouchi, H.; Sasada, Y. *Chem. Lett.* **1974**, *3*, 639.

(33) Kumar, V.; Wang, L.; Riebe, M.; Tung, H.-H.; Pud'homme, R. K. *Mol. Pharm.*, doi: 10.1021/np.90002t.

(34) Sieval, A. B.; Vlemming, V.; Zuilhof, H.; Sudholter, E. J. R. *Langmuir* **1999**, *15*, 8288.

(35) (a) Garcia-Garibay, M. A. *Acc. Chem. Res.* **2003**, *36*, 491–498. (b) Garcia-Garibay, M. A.; Shin, S.; Sanrame, C. *Tetrahedron* **2000**, *56*, 6729–6737.

(36) Ihmels, H.; Patrick, B. O.; Scheffer, J. R.; Trotter, J. *Tetrahedron* **1999**, 2171.

(37) Becker, H.-D.; Sandros, K.; Skelton, B. W.; White, A. H. *J. Phys. Chem.* **1981**, *85*, 2930.

(38) Becker, H.-D.; Andersson, K. *J. Org. Chem.* **1987**, *52*, 5205.

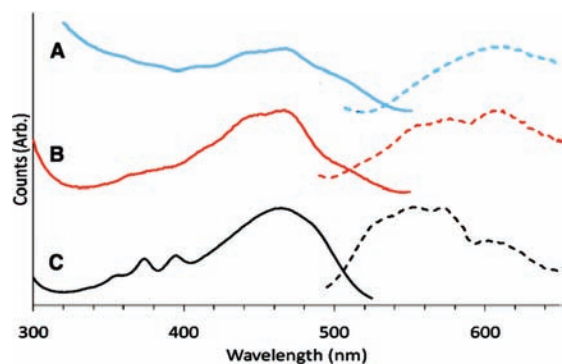


Figure 2. Excitation and emission spectra of dianthryl cyclopropanone **1g** in CH_2Cl_2 (C, black) and in an aqueous suspension (B, red). Excitation and emission spectra of dianthryl acetylene **2g** in an aqueous suspension (A, blue).

could be due to trace amounts of dianthryl acetylene **2g** acting as a very efficient quencher. However, the absorption spectrum of **2g** has a poor spectral overlap with emission of **1g**. Furthermore, samples of **1g** irradiated (at 266, 350, or 480 nm) for 2 h did not show changes in the emission envelope or intensity that could be associated with the involvement of **2g** by direct excitation or as an energy acceptor. It should be pointed out that a modest increase in intensity could have been expected on the basis of the fact that the fluorescence quantum yield of **2g** ($\Phi_F = 0.04$)³⁹ is about 4 times greater than that determined here for **1g** ($\Phi_F = 0.01$). We conclude that the solid-state reaction of **1g** is not prevented by product quenching.

Nanometer-Scale Mechanical Response of DPCP Crystals to the Solid-State Reaction. We previously reported in situ microscopic observation of large specimens of DPCP crystals exploding and crumbling into a fine powder of DPA after a few minutes of UV irradiation.¹⁹ We suggested that such a remarkable mechanical response may be the combined result of the very fast reaction, which does not allow for local relaxation, and the large changes in volume that take place at the molecular level when bent molecules of DPCP transform into linear molecules of DPA and CO.⁴ Given that the mechanical response of several photoreactive crystals has been shown to depend strongly on their initial size,^{40,41} we became interested in documenting such effects at the nanometer scale when dry DPCP crystals are irradiated and in determining whether a similar effect would take place with nanocrystalline specimens in water suspensions.

To explore the nature of the reaction at the nanometer scale, we drop-cast a sample of DPCP on an alkane-terminated Si wafer and observed the edges of the relatively large crystal specimens by AFM in a tapping mode (Figure 3a). The AFM image obtained after the same sample was irradiated for 10 min with a Xe lamp with $\lambda > 300$ nm revealed a remarkable transformation (Figure 3b). The resulting DPA is seen as a collection of individual nanocrystals with an average diameter of ca. 40 nm. Complementary experiments to investigate changes in crystal size for nanocrystalline suspensions as a function of conversion were analyzed by DLS with a sample of DPCP analyzed before and after exposure to UV light for several time intervals. The DLS results showed that the average crystal

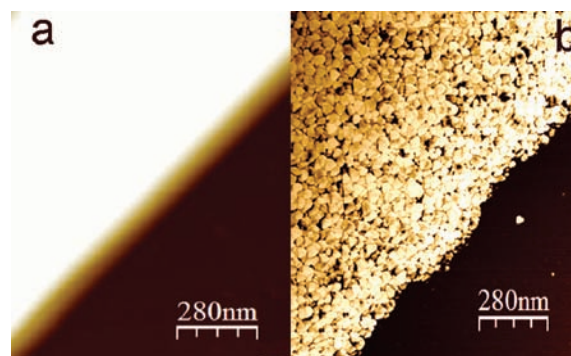


Figure 3. AFM images of the edge of a DPCP crystal on an alkene-functionalized Si surface (a) before exposure to light and (b) after 10 min of irradiation with a Xe lamp with $\lambda > 300$ nm.

size in a given sample decreased from ca. 1200 nm before irradiation to ca. 200 nm after 40% conversion. However, further irradiation and continued conversion did not result in a further decrease in the average particle size. The large crystal size of the initial suspension in this case was selected to show a greater size change and was obtained by preparing a sample with a higher DPCP loading. In conclusion, while it is clear that the reaction results in a remarkable process that leads to recrystallization of the product in specimens of very small size, it is not known at this time whether the final dimension is determined by initial crystal size or by differences arising from the sample being suspended in water versus at a dry air–crystal interface.

Quantum Yield Determinations in Solution. The UV spectrum of DPCP is characterized by a very weak S_0 – S_1 transition between ca. 330 and 390 nm, with $\lambda_{\text{max}} \approx 370$ nm and $\log \epsilon \approx 3.3 \text{ M}^{-1}\text{cm}^{-1}$, and a very strong S_0 – S_2 transition between 240 and 325 nm, with $\lambda_{\text{max}} \approx 300$ nm and $\log \epsilon = 4.28$ (284 nm), 4.33 (295 nm), and 4.16 (307 nm) $\text{M}^{-1}\text{cm}^{-1}$.^{2,3} Although the derivatives possess different shapes and λ_{max} values, it appears that differences in the intensity of the corresponding transitions also occur in the other DPCP derivatives. As indicated in Table 1, the solution quantum yields for derivatives **1c**, **1d**, **1f**, and **1g** after excitation at 350 nm, corresponding mainly to S_0 – S_2 transition, have been reported in the literature. The quantum yields of **1b**, **1e**, **1i**, and **1j** were determined in this study by standard potassium ferrioxalate actinometry⁴² with excitation to the S_2 state (or higher) by irradiation at 312 nm. As shown in the table, the quantum efficiency for the parent DPCP is quantitative, with $\Phi_{\text{sol}} = 1.0$. Other compounds in the table can be classified in three groups. Compounds with 1-naphthyl (**1c**), 2-methoxy-1-naphthyl (**1e**), and 5-phenyl-2-methoxyphenyl (**1f**) groups have solution quantum yields that are $\Phi_{\text{sol}} \geq 0.5$. The second group comprises compounds with *p*-MeO (**1b**), *p*-(2-phenyl)ethyl (**1e**), *p*-hydroxy (**1i**), and *p*-phenoxy (**1j**) groups, which have $\Phi_{\text{sol}} \approx 0.2$. The third group includes the 9-anthryl-substituted analogue **1g**, which has unreactive low-energy states, and the *p*-iodo derivative **1i**, which provides a spin–orbit coupling mechanism that quenches the reaction. Compound **1g** has a very low reaction quantum yield of Φ_{sol}

(39) Makino, T.; Toyota, S. *Bull. Chem. Soc. Jpn.* **2005**, *78*, 917.

(40) Garcia-Garibay, M. A. *Angew Chem., Int. Ed.* **2007**, *46*, 8945.

(41) (a) Al-Kaysi, R. O.; Müller, A. M.; Bardeen, C. J. *J. Am. Chem. Soc.* **2006**, *128*, 15938. (b) Al-Kaysi, R. O.; Bardeen, C. J. *Adv. Mater.* **2007**, *19*, 1276.

(42) Murov, S. L.; Carmichael, I.; Hug, G. L. *Handbook of Photochemistry*, 2nd ed.; Marcel Dekker, Inc.: New York, 1993.

= 0.02, and **1i** is completely photostable. The reduced chemical efficiency of the substituted DPCPs in solution is indicative of slower decarbonylation reactions, faster internal conversion, and/or decay to the ground state. While information to assign the contributions to reactions from the S_2 and S_1 states is not available, suppression of the adiabatic reaction would completely eliminate a solid-state quantum chain. In contrast, even a fraction of molecules reacting along S_2 may be able to initiate a chain reaction that can be propagated by energy transfer from the excited product to the reactant. This was tested by quantum yield determinations in the solid state.

Quantum Yield Determinations in Nanocrystalline Suspensions. Quantum yield determinations in the solid state were carried out by chemical actinometry with nanocrystalline suspensions. Particle loadings were adjusted so that all the photons from the UV source are absorbed and can be accounted for. Having shown that dicumyl ketone (DCK) is a good nanocrystalline actinometer with a quantum yield of decarbonylation of $\Phi_{\text{DCK}} = 0.20$,⁴³ we set out to determine the quantum yield of decarbonylation for all the reactive DPCPs in Table 1 using mixed suspensions. Taking advantage of this method, we previously reported that the quantum yield of the parent DPCP in a nanocrystalline suspension is $\Phi_{\text{CP}} = 3.3$. The extent of reaction in each case was determined by ^1H NMR for the DPCP analogues and by gas chromatography for DCK. Every sample was analyzed in triplicate or quadruplicate, and results were obtained with standard deviations less than 10%. Using co-suspended DCK nanocrystals as an internal actinometer, the quantum yield of decarbonylation is given by the following equation,

$$\Phi_{\text{susp}} = (A_{\text{CP}}/A_{\text{DCK}})(N_{\text{DA}}/N_{\text{DC}})\Phi_{\text{DCK}} \quad (1)$$

where A_{CP} is the absorbance of the cyclopropenone, A_{DCK} the absorbance of dicumyl ketone, N_{DA} the number of moles of diarylacetylene formed from the corresponding cyclopropenone, and N_{DC} the number of moles of dicumene formed from DCK with a quantum yield $\Phi_{\text{DCK}} = 0.20$. After more than 80 experiments with variations that included suspension loadings and with or without surfactants at pre-micellar concentrations, we determined that $\Phi_{\text{susp}} = 3.30 \pm 0.35$ at 312 nm. Quantum yields of reactions carried out in solution or upon excitation to S_1 between $\lambda = 350$ and 390 nm gave values of 1.0. The solid-state quantum yield strongly supports the mechanism in Scheme 1, with an average of 3.3 molecules per photon in the chain. Analogous quantum yield studies with over 25 independent measurements each were carried out with the other diaryl cyclopropenone derivatives in Table 1. Notably, independent quantum yield measurements using DCK or the parent DPCP as the chemical actinometer gave identical results, making the data set internally consistent. The quantum yields determined in this manner range from 0.87 to 2.74, which are higher than the values measured in solution, and in all cases but for **1j**, the values are greater than 1.0, as required for the sought-after quantum chain. Notably, the reaction is tolerant to several changes in the chromophore, including oxygen, naphthyl substituents, and extended linear conjugation. A quantum yield less than 1.0 in the case of diphenolate salt **1j** was confirmed with inorganic sodium and potassium salts suspended in hexane, removing suspicions of quenching by some neutral triethylamine.

Quantum Yield Amplification. It is well known that the crystalline environment can change excited-state deactivation pathways, such as internal conversion, intersystem crossing, and fluorescence, potentially affecting the reaction quantum yields.⁴⁴ For that reason, changes in the quantum yields of decarbonylation in nanocrystalline suspensions (Φ_{susp}) should be analyzed in terms of chain propagation by energy transfer and also in terms of possible changes in reaction efficiencies within the crystal lattice, the latter determined by an intrinsic quantum yield Φ_{CL} .

We define the quantum yield amplification (QYA) as the ratio of the quantum yield in nanocrystalline suspension (Φ_{susp}) relative to the quantum yield in solution (Φ_{sol}),

$$\text{QYA} = \Phi_{\text{susp}}/\Phi_{\text{sol}} \quad (2)$$

Starting with equal moles of reactant as dissolved and solid samples, QYA represents the equivalents of additional photons needed in solution to produce the same moles of product as in the solid state. The QYA values for all the compounds in this study are included in Table 1 and are as high as 11.4 in the case of **1b**.

In general, the propagation length of a quantum chain reaction is determined by the fraction of molecules that proceed to the product in the first adiabatic reaction (e.g., Φ_{CL}) and which are involved in the subsequent energy-transfer step (Scheme 1). Notably, a quantum chain reaction does not imply a quantum yield greater than 1, even with an infinite number of energy-transfer steps. The quantum yield of a general chain reaction (Φ_{chain}) with n energy-transfer steps can be described by a geometric series of the form

$$\Phi_{\text{chain}} = (\Phi)^1 + (\Phi)^2 + (\Phi)^3 + \dots + (\Phi)^n \quad (3)$$

with the value of n determined by the relative rates of energy transfer and excited-state decay,

$$n = k_{\text{ET}}/k_{\text{dec}} \quad (4)$$

For a hypothetical solid-state reaction with an infinite number of energy-transfer steps ($n = \infty$) and an intrinsic quantum yield Φ_{CL} , the series converges to the limit

$$\Phi_{\text{chain}} = \Phi_{\text{CL}}/(1 - \Phi_{\text{CL}}) \quad (5)$$

which results in observed efficiencies in the ranges of

$$\Phi_{\text{chain}} < 1.0 \text{ for } \Phi_{\text{CL}} < 0.5$$

$$\Phi_{\text{chain}} = 1.0 \text{ for } \Phi_{\text{CL}} = 0.5$$

$$\Phi_{\text{chain}} > 1.0 \text{ for } 0.5 < \Phi_{\text{CL}} < 1.0$$

Intrinsic quantum yields of 0.2, 0.4, 0.7, 0.9, and 1.0 would give maximum Φ_{chain} values of 0.25, 0.66, 2.33, 9.0, and ∞ , respectively. The suspension quantum yields in Table 1 correspond to the quantum yield of the chain, i.e., $\Phi_{\text{susp}} = \Phi_{\text{chain}}$. In the case of **1b**, it can be seen that $\Phi_{\text{sol}} = 0.24$ is not large enough to produce $\Phi_{\text{susp}} = 2.74$; therefore, $\Phi_{\text{CL}} \neq \Phi_{\text{sol}}$. For $\Phi_{\text{susp}} > 1$, Φ_{CL} must be greater than 0.5. At the same time, the quantum yield of suspensions of **1a**, $\Phi_{\text{susp}} = 3.3$, may imply that $\Phi_{\text{CL}} < \Phi_{\text{sol}}$ or, more likely, that the number of energy-

(43) Veerman, M.; Resendiz, M. J. E.; Garcia-Garibay, M. A. *Org. Lett.* **2006**, *8*, 2615.

(44) Kol'chenko, M. A.; Kozankiewicz, B.; Nicolet, A.; Orrit, M. *Opt. Spectrosc.* **2005**, *98*, 681.

transfer steps (n) is limited. The suggested increase in the efficiency of the solid-state decarbonylation (Φ_{CL}) of **1b–1f** and **1h–1i** may be due to an acceleration of the adiabatic reaction or to a deceleration of the rate of internal conversion and decay, the latter being more probable.

If one views energy migration in solids as discrete events, the efficiency of energy transfer from the excited-state photoproduct to unreacted starting material is determined by the time constant of energy transfer, τ_{ET} , relative to the time constant of internal conversion, τ_{IC} , to the S_1 of DPA. Energy transfer from DPA to DPCP within a crystal should take place within time scales typical of singlet exciton hopping, $\tau_{\text{ET}} \approx 1\text{--}2$ ps. The energetics for energy transfer are favorable (95 and 88 kcal/mol for the respective S_2 states), and translation symmetry of nearest neighbors guarantees van der Waals contacts and ideally parallel orientations. Given that the S_2 lifetimes of diarylacetylenes **2a**, **2b**, and **2i** in hexane solution reported by Hirata and Okada fall within $\tau_{\text{IC}} \approx 7\text{--}8$ ps,⁴⁵ one may expect that the average number of energy steps will be given by

$$n = k_{\text{ET}}/k_{\text{IC}} \approx 4\text{--}8 \quad (6)$$

Satisfyingly, the observed Φ_{susp} values are consistent with the estimated number of discrete energy transfers.

Conclusions

The photoinduced decarbonylation of diarylcyclopropenones to diarylacetylenes occurs with remarkable efficiency in the crystalline solid state. With a set of 10 aryl-substituted derivatives, we have shown that the adiabatic reaction previously postulated for the second excited state (S_2) of the parent diphenyl compound is capable of initiating a quantum chain process where the excited-state S_2 photoproduct transfers its energy within a few picoseconds to a ground-state reactant to propagate the chain. While the quantum yields of photodecarbonylation in solution vary from ca. 0.2 to 1.0, the values obtained with nanocrystalline suspensions vary from 0.87 to 3.3. The increase in quantum efficiencies on going from solution to crystalline solids corresponds to quantum chain amplification factors varying between 3.2 and 11.4. A remarkable mechanical response of the previously documented solid-to-solid reaction of diphenyl cyclopropenone **1a**, where large single-crystalline specimens turn into fine powders, was shown to scale down to the nanometer scale by formation of isolated crystalline specimens of the photoproduct of ca. 35 nm in size. Thus, the remarkable potential of crystalline-state adiabatic photoreactions for chemical amplification has been unveiled with a very challenging system where the quantum chain is limited by the very short lifetime of an upper singlet excited state. Future femtosecond spectroscopy measurements with nanocrystalline suspensions of the DPCP analogues **1a–1i** should help to firmly elucidate the kinetics of the reaction and the operative energy-transfer mechanism and to elucidate the factors that determine the solution quantum yields. Current work by our group is aimed at studies involving adiabatic reactions that occur in the triplet state which, according to triplet-state lifetimes and known energy-transfer efficiencies, could be

expected to give rise to millions of product molecules per photon of light absorbed by the crystalline reactant.

Experimental Section

General Methods. Solid-state ^{13}C NMR spectra were acquired on a Bruker DRX300 instrument. IR spectra were obtained with a Perkin-Elmer Spectrum instrument equipped with a universal attenuated total reflectance (ATR) accessory. Gas chromatography data were acquired on a Hewlett-Packard 5890 series II gas chromatograph equipped with an HP3396 series II integrator and an HP-5 capillary column of dimensions 25 m \times 0.2 mm with a film thickness of 0.11 mm. The excitation and emission spectra of all samples were obtained on a Photon Technology International Quanta Master spectrofluorimeter. Dynamic light scattering measurements were taken on a Beckman-Coulter N4 Plus submicron particle size analyzer. Silica used for purification was Silica-P flash silica gel (40–62 Å), purchased from SiliCycle Inc. UV–vis spectra were taken on a Beckman DU-650 spectrometer.

Nanocrystalline Suspensions. Nanocrystalline suspensions for microscopy and DLS studies were prepared by injecting 50 μL of a DPCP (8 mM) solution in acetone into 10 mL of vortexing water (Millipore). The resulting suspension (4×10^{-5} M) was sonicated three times at room temperature for 4 min, allowing for 2 min rest between runs. These samples were not made using surfactant. During drying, the drop-cast suspension will become more concentrated. If CTAB is present in the suspension, its concentration will eventually rise above the critical micelle concentration. The formation of micelles or the observation of CTAB is undesirable in this situation; therefore, surfactant was not used during the microscopy studies. AFM studies were performed in tapping mode with a multi-mode Veeco Nanoscope IIIa instrument using monolithic silicon probes with a tip radius reported to be <10 nm (VistaProbes T300R, Nanoscience Instruments, Inc., Phoenix, AZ). To prepare the AFM sample, a dilute DPCP suspension (4×10^{-5} M) was drop-cast onto a clean silicon wafer and allowed to dry in a desiccator. Scanning electron microscopy studies were performed with a JEOL JSM-6700F field-emission scanning electron microscope. To prepare the SEM sample, a dilute DPCP suspension (4×10^{-5} M) was drop-cast onto carbon tape and allowed to dry in a desiccator.

Relative quantum yield determinations were performed with dicumyl ketone as an internal standard in a Rayonet photochemical reactor using either 312 nm lamps (BLE-8T312) or 352 nm lamps (BLE-8T352). Quantum yields were determined with equimolar, optically dense suspensions. Two independent suspensions of actinometer and substrate were independently synthesized. They were then combined immediately prior to irradiation in a 50 mL quartz Erlenmeyer flask and irradiated for 5 min. Every minute, an aliquot was removed (approximately one-fifth of the suspension). The suspensions were extracted with deuterated chloroform (2 mL), washed with brine (2×2 mL), and dried over magnesium sulfate. ^1H NMR spectra were taken immediately to determine the extent of product formation. In the case of **1g**, due to insolubility in chloroform- d_3 , the suspensions were evaporated under a stream of argon at room temperature and ambient pressure. The residue was dissolved in methanol- d_4 for ^1H NMR analysis.

The same samples were then subjected to gas chromatography to determine the extent of dicumyl formation. The conversion of cyclopropenone derivatives (CPD) could not be monitored by gas chromatography due to partial thermal decarbonylation that occurred. Many of the CPD were not thermally stable at elevated temperatures. DPCP has been shown to thermally decarbonylate between 130 and 140 $^\circ\text{C}$.⁴⁶ Thermal decarbonylation was noted in all cases for the CPD when subjected to gas chromatography to give the acetylene exclusively. Therefore, gas chromatography was not used to detect DPCP/CPD conver-

(45) Hirata, Y.; Okada, T *Chem. Phys. Lett.* **1993**, *209*, 397.

sion. It was confirmed that, at 60 °C, the cyclopropenone moiety is stable and does not thermally decarbonylate.

These experimental yields were reproduced at least in triplicate with CTAB/H₂O. High conversion data were not used to avoid potential problems caused by the absorption of the products.

Acknowledgment. Financial support by the National Science Foundation (Grants DMR0605688 and CHE0551938) is gratefully

acknowledged. G.K. acknowledges the National Science Foundation IGERT MCTP Program (DGE0114443).

Supporting Information Available: Synthetic procedures and spectral characterization of all compounds; solid-state analysis (XPD, DSC, and DLS) of **1a** as a function of the reaction progress in the solid state. This material is available free of charge via the Internet at <http://pubs.acs.org>.

JA9043449

(46) Breslow, R.; Haynie, R.; Mirra, J. *J. Am. Chem. Soc.* **1959**, *81*, 247.